

OPTICAL DETERMINATION OF CONSTITUTIVE EQUATIONS PARAMETERS OF NONLINEAR MATERIALS

Daniel Vavřík¹, Jan Korouš¹, Jaroslava Zemánková¹, Petr Jaroš²

Abstract

The paper presents simple optical experimental method for determination of constitutive equations parameters of nonlinear materials. Usually only one extensometer or strain gauge is used for the determination of strain in loading direction and one for the determination of a contraction in standard tensile test. It is necessary to have a number of the specimens for determination of constitutive equation for nonlinear material behaviour. Optical observation gives us the possibility to determine strain and contraction in large region of test specimen. It is possible to use only one specimen with this technique. On other hand, it isn't too easy to determine material parameters of hyperelastic material with standard experimental techniques but optical method provide number of experimental results in simple way.

Key words: Optical experimental method, Grid method, Nonlinear fracture mechanics, Gurson-Tvergaard damage model.

Introduction

Gurson-Tvergaard damage model is widely used nowadays in nonlinear fracture mechanics. This approach, so-called „local approach“, has been the subject of many research activities in the recent years. It has been shown that the local approach provides a complementary approach to the conventional fracture mechanics methods and may be used when crack growth simulation is required. A critical aspect of this approach is an accurate assessment of the local void parameters in volume by using experimental calibration procedures [1].

A methodology was developed for adjusting the parameters of the Gurson-Tvergaard model using the simulation of axisymmetrical notched tensile specimens. Notched tensile specimens offer the advantage of obtaining a very extensive zone affected solely by nucleation, which allows this parameter to be well adjusted. The process of parameter adjustment must be carried out in the number of specimen with different geometric configurations to determine the effect of the stress triaxiality on these parameters [2]. New approach to this problem was developed in the Institute of Theoretical and Applied Mechanics. Black lines were created on axisymmetrical notched tensile specimens (see *Fig. 1.*) with collaboration with Techlab² (Prague company).

¹ Ing. Daniel Vavřík, Ph.D., Ing. Jan Korouš, Ing. Jaroslava Zemánková, CSc., Ústav teoretické a aplikované mechaniky AV ČR, Prosecká 76, 190 00, Praha 9, tel. 02/86882121, e-mail: vavrik@itam.cas.cz , korous@itam.cas.cz , zemankova@itam.cas.cz

² Ing. Petr Jaroš., Techlab, s.r.o., Sokolovská 207, 190 00, Praha 9, tel. 02/83890581, e-mail: techlab@czn.cz,

The lines were used as a measuring grid. Software developed using Matlab is able to detect the edges of the each line. Differences between unloaded and loaded specimen gives us tensile strain time evolution and contraction on each line.

Each measuring line corresponds to different diameter of the specimen. This model may be seen equivalent to number of the specimens with different cross-area. Therefore, in our case we obtained experimental data from ten grid lines.

This methodology is useful also for determination of material parameters of other mechanical problems, like determination of material parameters of hyperelastic materials.

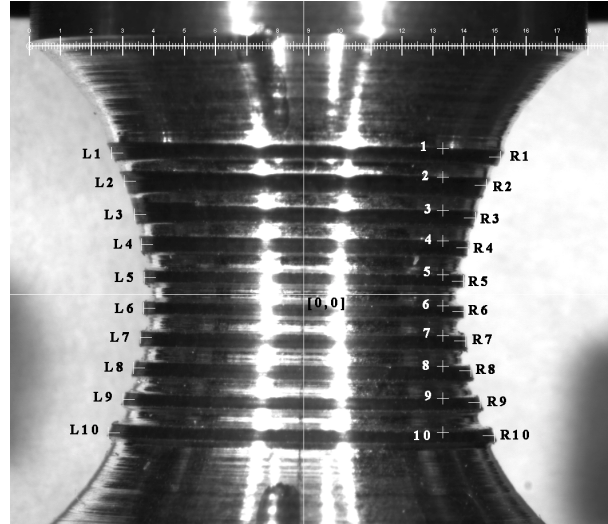


Fig. 1: Geometry of specimen. Diameter of a bar is 18 mm. Radius of the notch is 12 mm. Measuring points determined by image data processing are drawn in the picture.

Experimental setup

The specimen was observed by a black-and-white digital CCD camera with resolution 1200x1000 pixel. Frame rate of this camera is 25 frames/sec. Used macro-lens has small optical angle and high resolution. This lens has the telecentric behaviour in used magnification. The loading force was recorded from the loading machine. Time was used as a scale for later processing.

Data storage

One frame represents 767 kB with above mentioned resolution. It means almost 20 MB per second. It is impossible to record whole experiment with the full camera frame rate on PC HD. So, one frame was continuously saved on the HDD every second. Data from the last 5 seconds were recorded in the full frame rate and stored in the RAM buffer. The RAM buffer was written on the HDD at the end of the experiment.

Duration of the whole experiment was 564 sec and 168 frames were analysed.

Determination of strains and contractions on the measuring lines

Tensile strains were solved as follows:

$$\varepsilon_{11}(i) = \frac{(line_edge_t(i+1) - line_edge_t(i)) - (line_edge_0(i+1) - line_edge_0(i))}{(line_edge_0(i+1) - line_edge_0(i))} \quad (1)$$

Where $line_edge$ represents the vertical coordinate of the measuring line edge. The index i corresponds with the measuring line number (see Fig. 1.), the index t represents the actual experiment time and the index 0 corresponds with the unloaded specimen stage.

Vertical coordinates of the measuring line edges were identified in two steps:

1. Position of the measuring line centres

Data that represent grey level in the vertical profile (averaged by 61 columns) were interpolated by a quadratic polynomial function in the sliding window. This profile goes

thought points numbered by 1-10 in Fig.1. The scale of the sliding window determines the scale of peaks, which should be localized. Extremes of ten interpolating polynomial function with the highest first constant correspond to positions of the measuring lines. On our specimen ten measuring lines have been done.

Eleven interpolating function with the lowest first constant of the polynomial function correspond to the position of the gaps between the measuring lines.

2. Position of the edges of one measuring line

The data between line and gap position were interpolated by a linear polynomial function in the sliding window. The scale of the sliding window determines the scale of the slope, which should be localized. Interpolating polynomial function with the highest first constant correspond to the sliding window position on which maximal derivation is expected. Data in the determined window were interpolated by a polynomial function of the 3rd order. The interpolation function inflex point should be the expected position of the line edge.

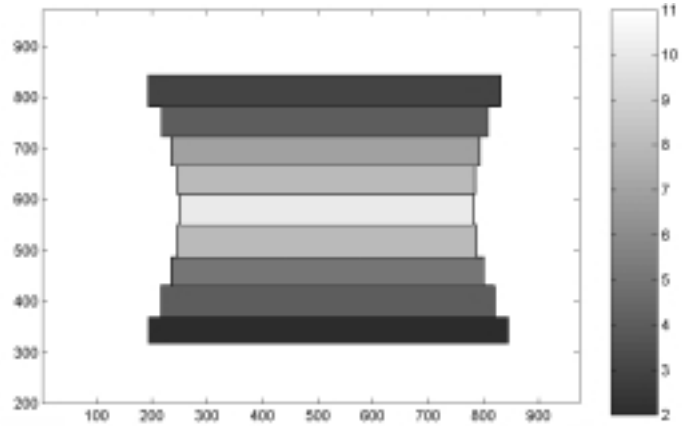


Fig.2: Tensile strain on the specimen 1/25 sec before failure.

Contractions were solved similarly as tensile strains:

$$\varepsilon_{22}(i) = \frac{(spec_edge_i(i+1) - spec_edge(i)_i) - (spec_edge_0(i+1) - spec_edge(i)_0)}{(spec_edge_0(i+1) - spec_edge_0(i))} \quad (2)$$

Where $spec_edge$ represents the horizontal coordinate of the specimen edge in the measuring line position.

Horizontal coordinate of the specimen edges in the measuring line position were identified as follows:

Data that represent grey level in the horizontal profiles (averaged by 3 rows) were interpolated by a linear polynomial function in the sliding window. These profiles go through points labelled by $Li-Ri$ in Fig.1, where i is measuring line number. The scale of the sliding window determines the scale of slope, which should be localized. The interpolating polynomial function with the highest first constant corresponds to the sliding window position on which maximal derivation is expected. Data in one window were interpolated by a polynomial function of the 3rd order. Its inflex point is the expected position of the line edge.

Gurson-Tvergaard Needleman model

For description of metal materials containing voids, the so-called Gurson model [3] is often used. There are many modifications of this model but a simple form was applied in this paper, the Gurson-Tvergaard-Needleman model.

Originally, the constitutive model was derived from a cell of material containing a void. The homogenous material surrounding the void is called as matrix material. Using the relation for

behaviour of a spherical void in a remote macroscopic stress and strain field according [4], Gurson described the yield condition in the form:

$$g(\sigma_e, \sigma_m, \bar{\sigma}, f) = \left(\frac{\sigma_e}{\bar{\sigma}}\right)^2 + 2q_1 f \cosh\left(\frac{3q_2 \sigma_m}{2\bar{\sigma}}\right) - (1 + q_3 f^2) \quad (3)$$

Where σ_e is the von Mises equivalent macroscopic stress, σ_m is the mean macroscopic stress, $\bar{\sigma}$ is the current yield stress of the matrix material and f denotes the current void fraction. Constants q_1 , q_2 and q_3 have been introduced by Tvergaard [5] in attempt to improve the model behavior.

The void evolution, i. e. the voids nucleation and growth, is described by equation:

$$df = df_{growth} + df_{nucleation} \quad (4)$$

The eq. (4) consists from two parts where df_{growth} gives the relation for growth of the existing voids whereas $df_{nucleation}$ enables to take into account nucleation of new voids. Following expressions are usually used:

$$df_{growth} = (1 - f)d\varepsilon_{kk}^p \quad (5)$$

$$df_{nucleation} = Ad\varepsilon^p \quad (6)$$

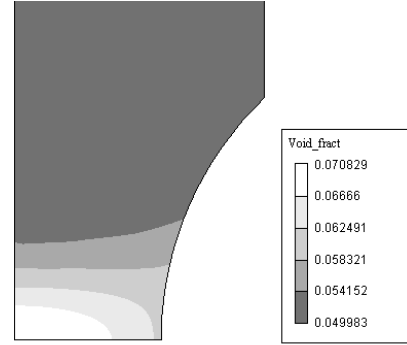


Fig.2: Fraction of voids coming from Gurson-Tvergaard-Needleman damage model for loading $F=38.67$ kN.

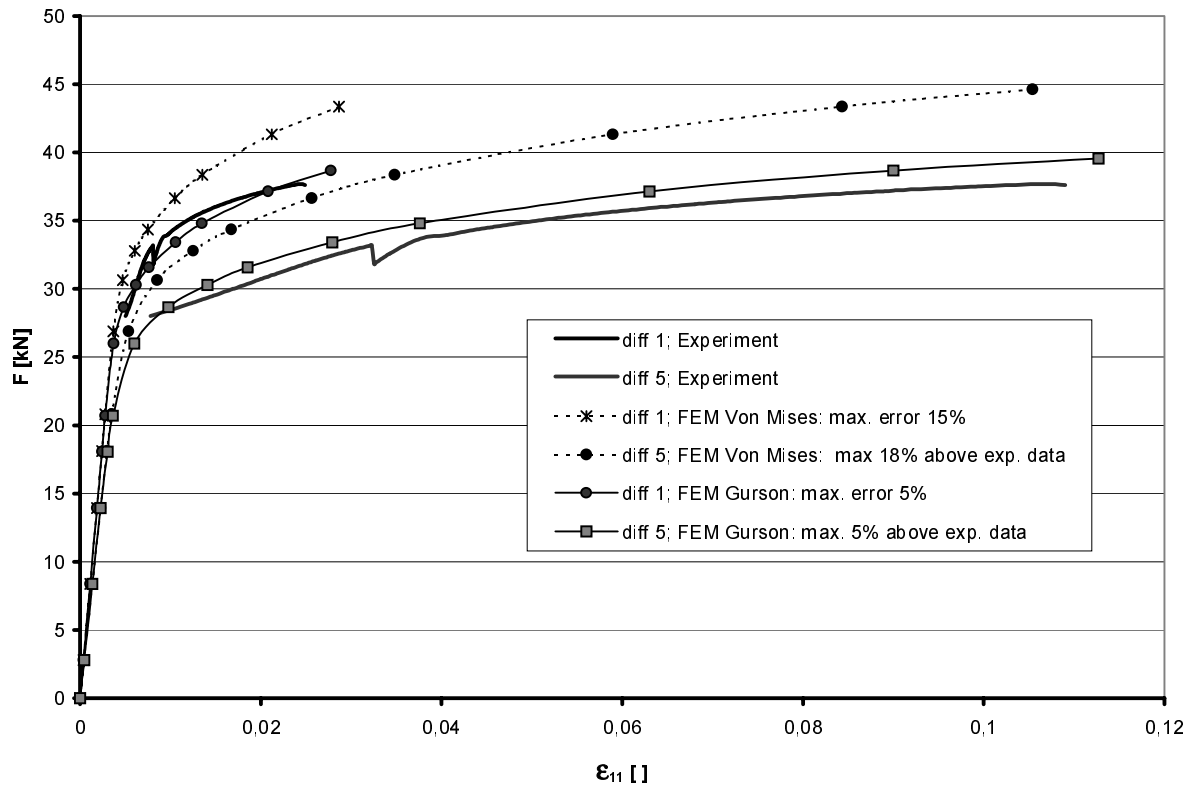


Fig. 4: Dependence “Tensile strain–Loading force” is drawn in the figure for the first difference (between first and second measuring line) and for middle difference (between fifth and sixth measuring line). Experimental and FEM results are compared.

where $d\epsilon_{kk}^p$ denotes the trace of the increment macroscopic plastic strain tensor and ϵ^p is the equivalent matrix plastic strain. Parameter A can be a function of the matrix stress and strain. In this paper, the relation according Chu and Needleman [6] was used:

$$A = \frac{f_N}{s_N \sqrt{2\pi}} \exp \left[-\frac{1}{2} \left(\frac{\epsilon^p - \epsilon_N}{s_N} \right)^2 \right] \quad (7)$$

Constants f_N , s_N , and ϵ_N are material constants. Several combinations of these parameters were tested.

Note, that in all analysed cases, the coalescence of voids was not taken into account. For the calculations, the program WARP3D [7] was used. The macroscopic plastic strains was calculated using flow rule associated with the condition (3):

$$d\epsilon_{ij}^p = d\Lambda \frac{\partial g}{\partial \sigma_{ij}} \quad (8)$$

where σ_{ij} are the macroscopic stress tensor components. The integration of the plastic strain rate over the step was performed using backward Euler procedure.

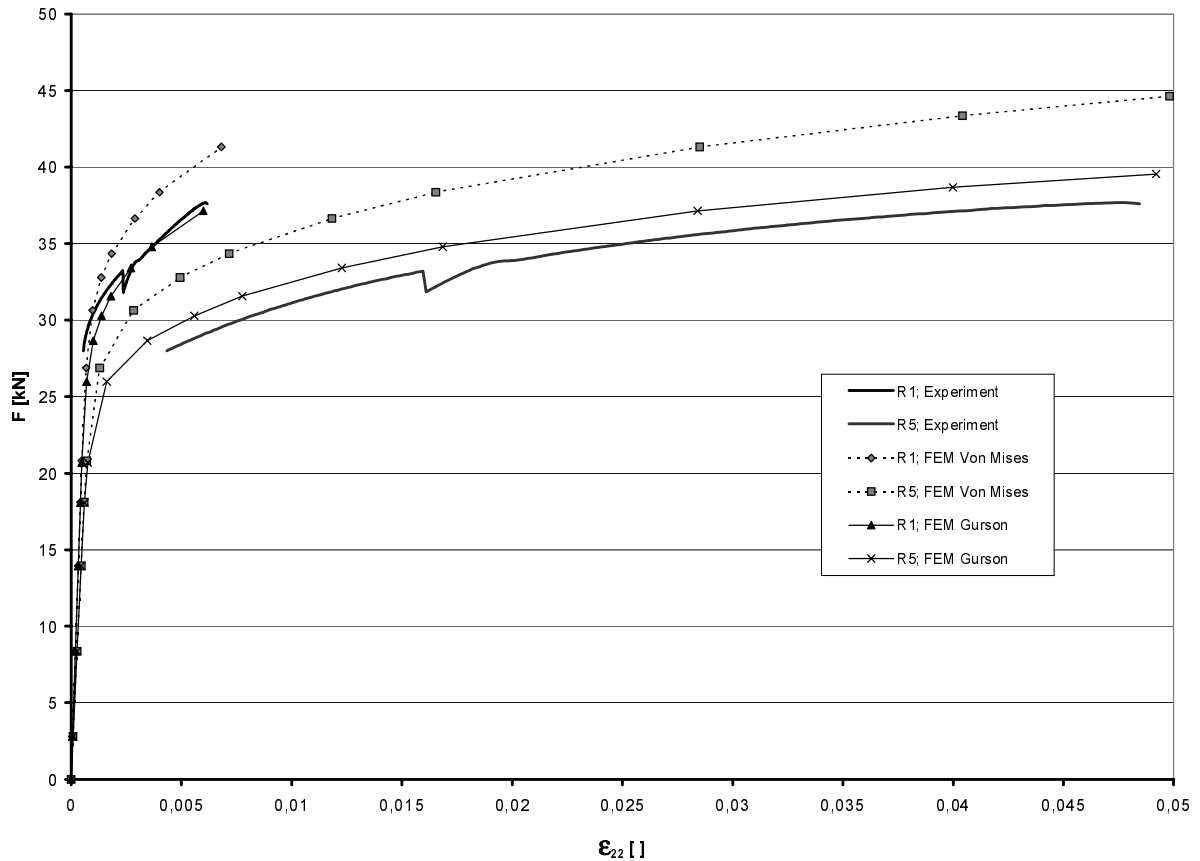


Fig. 5: Dependence “contraction–loading force” is drawn in the figure for the first measuring line (No.1) and for middle measuring line (No.5). Experimental and FEM results are compared.

Conclusions

- The method is able to provide large number of data for numerical simulation.
- No extra laboratory conditions are needed (in comparison with interferometric optical methods).
- Fully automatic image processing was used (168 frames were analysed).
- The experimental and FEM numerical results have good correlation (see *fig. 4* and *fig. 5*).
- The comparison between the numerical simulations based on “classical” von Mises material model and Gurson-Tvergaard damage model shows significant advantage of Gurson-Tvergaard model. This model will be used for numerical simulations of nonlinear fracture problems.
- This methodology is useful also for determination of material parameters of other mechanical problems. This optical method was used for “Experimental Determination of Constitutive Equation of Hyper-elastic Material” for instance [8].

Acknowledgement

This paper deals with the experimental part of the project 106/99/1467: “Thermodynamic Identification of Instabilities of the Cracked Body Subjected to Static Loading“ and project 106/00/D064: “Experimental investigation of the damage in ductile materials by voids evolution using an X-ray and fast position sensitive pixel detector system”. Both project are supported by the Grant Agency of the Czech Republic.

References

- [1] G. Shatil, L. Wang: *The Dependency of the Local Approach to Fracture on the Calibration of Material Parameters*, 13th European Conference on Fracture, 6-9 September, 2000, Spain.
- [2] J. M. Alegre, J. Pérez...: *The Application of the Gurson-Tvergaard Model in the Aging Embrittlement of Austeno-ferritic Stainless steels*, 13th European Conference on Fracture, 6-9 September, 2000, Spain.
- [3] A. L. Gurson: *Continuum Theory of Ductile Rupture by Void Nucleation and Growth: Part 1 – Yield Criteria and Flow Rules for Porous Media*, Journal of Engineering Materials and Technology, Vol. 99, 1977, pp. 2-15
- [4] J. Rice, D. M. Tracey: *On the Ductile Enlargement of Voids in Triaxial Stress Fields*, Journal of Mechanics and Physics of Solids, Vol. 35, 1968, pp. 379-386
- [5] V. Tvergaard: *Material Failure by Void Growth to Coalescence*, Advances in Applied Mechanics, Vol. 27, 1990, pp. 83-151
- [6] C. C. Chu, A. Needleman: *Void Nucleation Effects in Biaxially Stretched Sheets*, Journal of Engineering Materials and Technology, Vol. 102, 1980, pp. 249-256
- [7] A. S. Gullerud, K. C. Koppenhoefer, A. Roy, R. H. Dodds Jr.: *WARP3D: 3-D Dynamic Nonlinear Fracture Analysis of Solids Using Parallel Computers and Workstations*, Structural Research Series (607), UILU-ENG-95-2012, University of Illinois at Urbana-Champaign, (2000)
- [8] Jaroslav Kult, Daniel Vavřík: *Experimental Methods Used for Improvement of the Computational Model of Silicon Rubber Implant*, Proceedings of EAN 2001, Tábor, 2001